A low-temperature ultrahigh vacuum scanning tunneling microscope with a split-coil magnet and a rotary motion stepper motor for high spatial resolution studies of surface magnetism

O. Pietzsch,[a] A. Kubetzka, D. Haude, M. Bode,[b] and R. Wiesendanger
Institute of Applied Physics and Microstructure Research Center, University of Hamburg, Jungiusstr. 11, D-20355 Hamburg, Germany

(Received 17 August 1999; accepted for publication 6 November 1999)

We present the design of a new ultrahigh vacuum scanning tunneling microscope (STM) which operates at $T<20$ K inside the bore of a 2.5 T superconducting split-coil magnet. The tip/sample region can easily be controlled visually, thus allowing safe and fast exchange of samples and tips while the microscope stays at low temperatures. A newly developed rotary motion stepper motor is presented which allows rotation of the sample by $>270°$ about an axis perpendicular to the tip axis. This feature allows metal or molecular beam evaporation normal to the sample surface. Even more important, by means of this device tip and sample can be brought into a parallel or antiparallel magnetic configuration thus opening a novel approach to the study of magnetic phenomena on an atomic length scale. In addition, measurements of the magneto-optical Kerr effect can be carried out without removing the sample from the STM. Also a new tip exchange mechanism is described. The microscopic and spectroscopic performance of the new instrument is illustrated on Au(111)/mica, on Tb(0001)/W(110), and on Gd(0001)/W(110). © *2000 American Institute of Physics.* [S0034-6748(00)04202-7]

I. INTRODUCTION

Micro- and nanomagnetism has been a subject of highly increased interest during the last decades. A great variety of phenomena is encountered when magnetic properties are studied under the condition of reduced dimensionality as, e.g., in ultrathin films. Although considerable experimental and theoretical progress has been achieved in the last few years the subject matter is mainly still in the field of basic research. It is a unique situation that, despite the fact that many riddles still have to be solved, certain technological applications already have reached the mass market, the perhaps most prominent example being IBM's new hard disk read/write head which is based on the only recently discovered giant magnetoresistance effect.[1–3] Driven by the demand for ever higher data storage and processing capacity there is an increasing request for nanotechniques that promise to be able to tailor magnetic materials exhibiting well defined properties. Prerequisite is, however, a better understanding of magnetic order on a nanometer scale, ultimately at the atomic level.

Conventional magnetic imaging techniques such as magneto-optical Kerr effect (MOKE) microscopy have provided valuable insight into surface magnetism. The spatial resolution of MOKE, however, is limited to about 300 nm by the wave length of the probing light. It is clear that the received signal is an average over the respective surface fraction. MOKE has been employed in scanning near-field optical microscopy (SNOM) in order to circumvent this limitation. A spatial resolution of approx. 50 nm has been obtained so far.[4] Scanning electron microscopy with polarization analysis (SEMPA) is another high resolution magnetic imaging technique. The lateral resolution limit is about 40 nm up to date.[5] In magnetic force microscopy (MFM) the external magnetic stray field of the sample is probed. Due to this long range interaction again the lateral resolution is limited and comes down to 20–50 nm.[6]

Scanning tunneling microscopy (STM) and its derivative scanning force microscopy (SFM) are the only techniques providing real space images of atomically resolved surfaces. Beside this well known atomic resolution capability STM can be used in spectroscopic modes to attain detailed energetically resolved information on the electronic properties of the surface under study near the Fermi level. Moreover, a scanning tunneling microscope sensitive to the spins of the tunneling electrons is ideally suited to investigate the correlations of topographic, electronic, and magnetic properties on an atomic length scale. In the past, two different experimental concepts have been applied to achieve spin-polarized vacuum tunneling:

(1) Ferromagnetic probe tips were used to map the local differential conductivity difference for parallel ($\uparrow\uparrow$) or antiparallel ($\uparrow\downarrow$) spin configurations of tip and sample (spin valve effect).[7,8]
(2) Optically pumped GaAs tips have been used to image the magnetic domain structure of thin Co films.[9]

Spin-polarized STM studies are extremely rare up to date.[7–11] This is due partly to certain technical difficulties (e.g., one needs a reliable *in situ* tip exchange mechanism in order to compare measurements taken with ''normal'' tips to

[a]Author to whom correspondence should be addressed; electronic mail: pietzsch@physnet.uni-hamburg.de
[b]Electronic mail: bode@physnet.uni-hamburg.de

those taken with ferromagnetic or GaAs tips), but the main problem is to clearly discriminate magnetically caused contrasts from those caused by other features of the electronic density of states near the Fermi level. A special problem is to determine the relative magnetic orientation (parallel or antiparallel) between the very end of the tip and the sample. As we will show below this problem can be solved by an experimental setup which provides an external magnetic field combined with the ability to rotate the sample without changing the tip position. Under these conditions any orientational relationship can be realized.

In the last decade a considerable number of low or variable temperature STMs have been developed. However, the number of instruments equipped with an external magnetic field is still very limited. At the University of Illinois at Urbana-Champain a variable temperature STM[12] for a temperature range of $1.5\,\mathrm{K}<T<300\,\mathrm{K}$ is installed which is operated in a 8 T magnet. Sample preparation is performed at high vacuum conditions (10^{-9} Torr). Reportedly, due to the long cooling time required (16 h) this instrument is limited to chemically inert samples. Another cryomagnet STM is installed at the University of Nijmegen (The Netherlands).[13] The working temperature is reported to be 1.5–4.2 K. The superconducting magnet supplies a magnetic field of up to 9.5 T. The STM has been designed to also fit into the 30.4 T hybrid magnet of the Nijmegen High Field Magnet Laboratory. Sample preparation at ultrahigh vacuum (UHV) conditions is not reported. At the University of Hamburg (Germany) a UHV low temperature (8 K) STM[14] is in use which is equipped with two superconducting magnets. One is a solenoid type capable of 7 T field strength perpendicular to the sample plane, the other one is a 2 T split pair type oriented parallel to the sample plane. By superimposing the fields of the two magnets a rotatable effective field of $B_{\max}=1\,\mathrm{T}$ can be created at the sample location. All stages of sample preparation can be performed *in situ*. Recently, a new design of a millikelvin STM with a 7 T superconducting magnet has been set up at the University of California, Berkeley.[15] Temperatures as low as 240 mK can be achieved. Fresh sample surfaces can be obtained by cleaving at low temperatures and thus at UHV conditions; further preparation facilities are not reported. Obviously, investigation of metal surfaces is not intended.

We have endeavored in designing a STM which is extremely stable and which meets three operational conditions: ultrahigh vacuum, low temperatures, and high magnetic fields. For the purpose of our special investigation in surface magnetism we have supplied the instrument with some unique features, like sample rotation, easy tip exchange mechanism, and an arragement for MOKE measurements.

II. CHAMBER SYSTEM

The new cryomagnet-STM chamber is added to a preexisting commercial four-chamber UHV system[16] consisting of a central distribution chamber, a preparation chamber equipped with resistive and electron beam heating and a sputter gun, a molecular beam epitaxy (MBE) chamber with five evaporators and a home built STM especially designed for time resolved growth studies described elsewhere,[17] an analysis chamber containing facilities for standard surface characterization as, e.g., low energy electron diffraction (LEED), Auger electron spectroscopy (AES) and spin-resolved photoelectron spectroscopy (SPPES), and, within an additional satellite chamber, a commercial variable-temperature STM[18] which can be operated in a temperature range of $30\,\mathrm{K}<T<380\,\mathrm{K}$. A load lock allows fast introduction of samples and tips without venting the chamber system. To prevent from acoustical and low frequency building vibrations the whole system is installed in an acoustically shielded laboratory with a foundation being completely separated from the rest of the building. The UHV chambers are supported by a table with additional pneumatic damping.

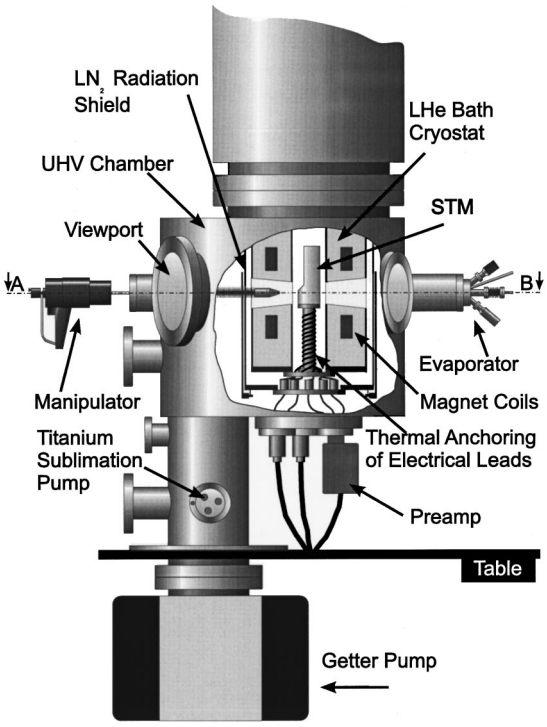

FIG. 1. (a) Schematic drawing of the cryomagnet STM system (side view). The STM is inserted from underneath through the base flange which also carries the electrical feedthroughs. For cut $A-B$ see Fig. 2.

III. MAGNET CRYOSTAT SYSTEM

A. Magnet

The magnet cryostat system (Fig. 1) is a modified Spectromag ^{4}He bath cryostat with a LN_2 radiation shield.[19] The 2.5 T superconducting magnet is a split coil type with a 62 mm bore. Homogeneity of the field in a 10 mm diameter spherical volume at the sample location is specified to 1 part in 10^2. The maximum sweep rate accounts to 2.5 T per minute. The central region of the magnet (cf. Fig. 2) has two cutaways of 80° and 90°, respectively, and a minimum height of 42 mm thus providing two access openings to the microscope. Samples and tips are being exchanged through the 80° window whereas the 90° window is used to carry out magneto-optical Kerr effect (MOKE) measurements, and to allow metal or molecular beam evaporation onto the sample surface.

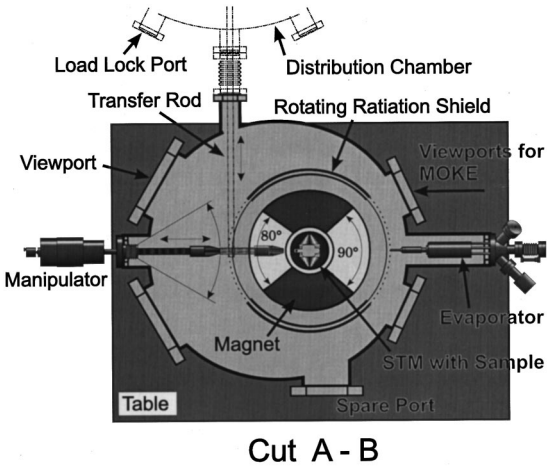

FIG. 2. Cut through the cryomagnet system at the sample plane.

To obtain proper UHV conditions the magnet is designed to safely endure bakeout at 120 °C. In our bakeout procedure we keep the magnet at 115 °C for 48 h. The temperature is measured by a platinum resistor sensor on top of the magnet. The signal of this sensor feeds a control unit that supplies a flow of cold nitrogen gas across the magnet if the temperature is about to surpass the set point value. Thus a safe bakeout operation is guaranteed over night.

B. Cryostat and UHV chamber

The helium reservoir of the cryostat has a useful capacity of 20 l giving a hold time in the low temperature regime of approx. 40 h between subsequent fills. The helium reservoir and the magnet are enclosed by a nitrogen radiation shield. Its 20 l volume provides a hold time of 36 h. At the lower end where the magnet has its above mentioned openings the shield has an additional rotating cylinder the purpose of which is to shut the access windows. This cylinder is thermically coupled to the main part of the shield by a number of copper braids.

To avoid vibrations due to boiling nitrogen the LN_2 reservoir is pumped to <5 mbar so that the nitrogen solidifies. To cope with the initially huge amount of gas from the boiling liquid we use a rotary vane pump with a nominal pumping speed of 65 m^3/h. When the nitrogen has solidified at a temperature of 63 K the rate of exhaust gas is greatly reduced so that a much smaller pump can be used to hold the pressure. This pump is located in an adjacent room which is acoustically isolated from the STM laboratory. As the gas flow through the pumping line is very low we have no acoustic coupling of the pump. Although approx. 30% of the nitrogen is lost at the first stage of this pumping procedure there is no substantial reduction of the hold time. Having a radiation shield at a temperature as low as 63 K is of considerable advantage for minimizing the helium boil off.

The outer vacuum chamber of the cryostat unit has a DN 350 CF base flange which fits onto the appropriate top flange of our custom-made UHV chamber. Pumping is done by a turbo pump, an ion getter pump, and a titanium sublimation pump. The base pressure after bakeout and cooldown is $<5\times10^{-11}$ mbar. The turn-around time for venting the system from low temperature, bakeout, and returning to low temperature, accounts to several days. Thus it is essential that samples and tips can be introduced through the load-lock of the central distribution chamber without breaking the vacuum.

IV. STM DESIGN

The design of the STM was geometrically restricted by the 62 mm diameter of the magnet's core tube. The cylindrical body of the STM, machined from one piece of the glass ceramic Macor,[20] has a diameter of 40 mm and a height of 110 mm. This body bears all parts of the microscope. It is mounted on top of an oxygen-free high-conductivity (OFHC) copper pedestal which serves both as the microscope's support and as the thermal anchoring for all electrical wirings. Together with this stand the microscope is installed as a unit into the magnet bore (cf. Fig. 3). To avoid any disturbance of the magnetic field the few metallic parts used are made from titanium, molybdenum, copper, or copper beryllium.

A. Approach mechanism

At the center of the microscope one finds two moving parts, the approach sledge bearing the scanner tube at its lower end [(b) in Fig. 4], and the sample receptacle (i) which can be rotated about the *y* axis. The coarse approach mechanism is based on Pan's design[21] that has proven to be stable enough to regain a microscopic location on the sample with an accuracy of less than 100 nm posterior to a macroscopic movement of 20 mm.[17,22]

The approach sledge is a polished sapphire prism placed in a V-shaped groove where it is rigidly clamped by two triplets of shear piezo stacks[23] [(c) in Fig. 4]. A 5mm$\times$5 mm $\times$1 mm Al_2O_3 pad is glued on top of each shear piezo stack. These pads provide the actual contact areas between the stacks and the sapphire prism surfaces. Two of the piezo stacks are glued to a Macor beam (d) which is pressed onto the prism by means of a molybdenum leaf spring (f) and a ruby ball (e). The Macor beam functions as a balance and thus warrants an equal distribution of the spring force to all contact areas of the six shear piezo stacks and the prism surface. In contrast to previously presented designs[14,15,24] we do not employ walker stepping as a working mechanism but use inertial movement by applying an asymmetric saw-tooth voltage curve to all six stacks simultaneously (stick slip). On the flat slope of the voltage ramp the prism follows the shear movement (stick) while, due to its inertial mass, it is unable to follow the rapid relaxation of the piezos on the steep slope (slip), the result being one step of the prism per period. The mechanism is driven at 0.5–1 kHz; the step size can be tuned by varying the applied voltage amplitude.

The scanner containing the tip is mounted to the lower end of the prism. The tip approach towards the sample to less than 0.5 mm distance is carried out manually using a remote control box; this operation can easily be controlled visually through one of the viewports with an *ex situ* located optical microscope. Only the fine approach is accomplished in automatic mode of the STM control unit. During a measurement the sapphire prism stays firmly clamped to the microscope

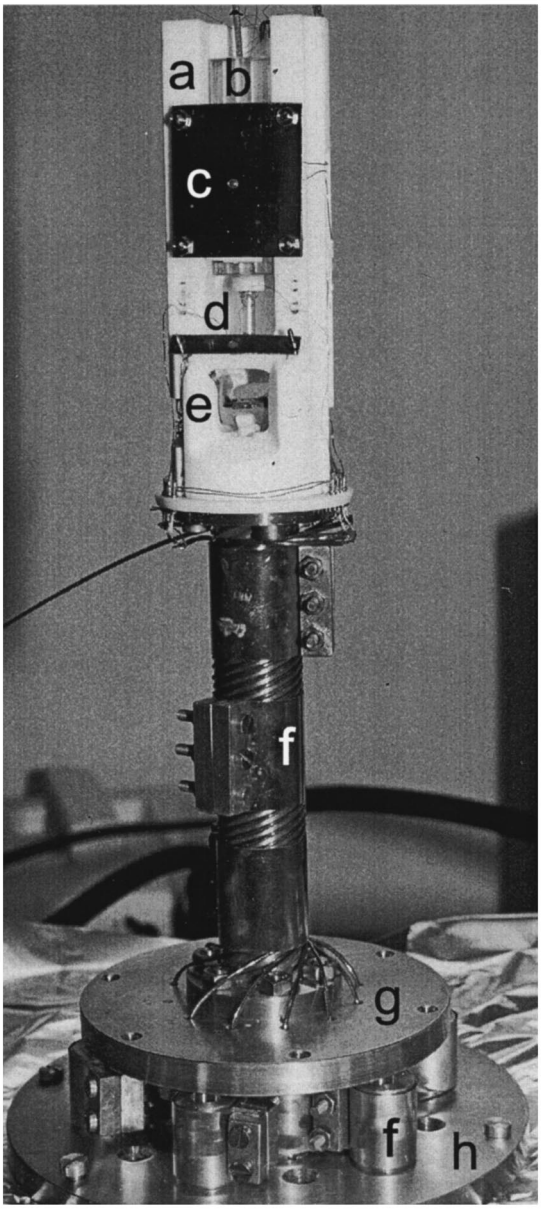

FIG. 3. Photograph of the microscope on its pedestal. (a) Macor body, (b) sapphire prism, (c) leaf spring, (d) tube scanner with tip, (e) sample, (f) thermal anchoring of electrical leads to helium and nitrogen temperature, respectively. When mounted to the cryostat the helium flange (g) and the nitrogen flange (h) are mechanically disconnected.

body. The scanner in use is a 1/4 in. EBL No. 4 piezo tube[23] with a length of 31 mm. This length was chosen in order to allow for a scan range of 5 μm at low temperatures (10.5 μm at room temperature) and still having a sufficiently high resonance frequency ($f_{\mathrm{res}}=2.2$ kHz). A great scan range is desirable for imaging of magnetic domains.

B. Sample rotation

The sample is introduced into a receptacle [(i) in Fig. 4] which can be rotated by more than 270° about the y axis. This rotor is a sapphire cylinder with the edges ground off to form two 90° cones. These cones are polished and again serve as the surfaces for stick-slip movement. In close analogy to the arrangement described above for the linear move-

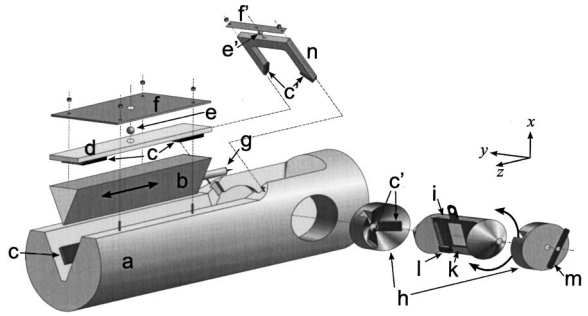

FIG. 4. Schematic drawing of the STM (not to scale). (a) Macor body, (b) sapphire prism, (c) and (c′) shear piezo stacks, (d) Macor beam, (e) and (e′) ruby ball, (f) and (f′) leaf spring, (g) scanner with tip, (h) stators for sample rotation, (i) rotor with sample, (k) spring, (l) temperature sensor, (m) leaf spring, (n) bridge.

ment there are six shear piezo stacks (c') two of which are pressed onto the cones by a bridge (n) with a leaf spring (f'). Due to the symmetry of this assembly it is self-centering in both radial and axial direction, and no additional bearings are required. When brought into place and turned for the first time the rotor, shaken by the rapid oscillatory piezo movements, takes on an equilibrium position and keeps it.

Between the two cones a recess is ground into the cylinder deep enough to receive the sample tray such that the sample surface lies in the $x-y$ plane. The sample tray is kept in place by a copper beryllium spring (k). The gap voltage to the sample is applied through a contact soldered to the spring. Also, the sample temperature sensor (l), a GaAlAs diode,[25] is glued onto the spring, and is thus in immediate proximity and in excellent thermal contact to the sample.

The capability to rotate the sample allows for some unique experimental arrangements, illustrated in Fig. 5. While the sample receptacle is in position (a) (i.e., the sample surface normal pointing in $+z$ direction) and the tip retracted, sample and tip exchange can be carried out. With the tip approached, this is also the position for STM measurements. After retraction of the tip a 90° rotation can be applied to the sample, thus turning the surface normal into the $-x$ direction [position (b)]. This position allows to direct

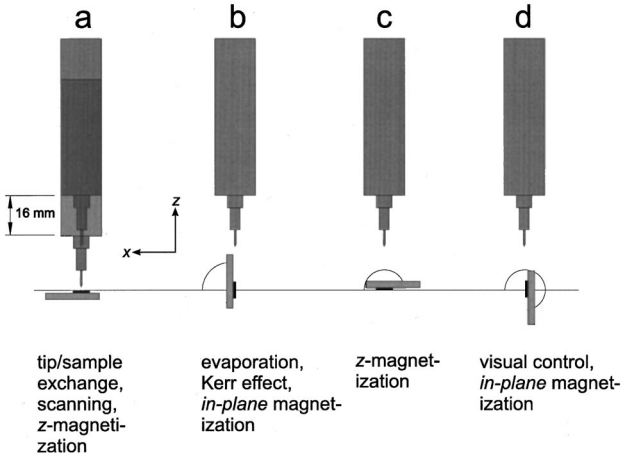

FIG. 5. Principal geometrical configurations of the sample. For details on the particular use of each position see text.

a molecular beam from the evaporator (cf. Figs. 1 and 2) to impinge normal to the sample surface. The sample rerotated back into position (a), STM imaging can, in principle, be applied for time resolved growth studies at low temperature and, if desired, in a magnetic field. Position (b) also allows for measurements of the magneto-optical Kerr effect (MOKE). The UHV chamber is supplied with two viewports at the appropriate sites (see Fig. 2), one for the incident beam, the other for the reflected beam.

C. Sample magnetization

Though the external magnetic field vector at the sample location is restricted to the z direction, the sample can be magnetized in almost any appropriate direction by virtue of the rotor. If in-plane magnetization is desired this can be achieved by turning the sample into position (b) or position (d), respectively. Out-of-plane magnetization is accomplished in positions (a) and (c). This latter configuration provides a very elegant way to study certain surface magnetic phenomena: Suppose a ferromagnetic sample being in position (c), and the external field applied in, e.g., the $+z$ direction. Having a ferromagnetic tip in use, both tip and sample will be magnetized according to the applied field. Now the field is switched off, and the sample is rotated by 180° into the scanning position, i.e., position (a). Tip and sample will now be in an antiparallel magnetic orientation. After taking a measurement in remanence the field is switched on again. The magnetization orientation of the tip will stay the same. The sample, however, will experience a reorientation of its magnetization, tip and sample magnetization thus ending up in a parallel configuration. With the external field switched off, again a measurement in remanence can be taken. Since, for the field sweep, the tip does not need to be retracted the second scan will image exactly the same location on the sample surface, thus allowing a one-to-one comparison of the two measurements.

D. Tip exchange mechanism

When working with ferromagnetically coated tips it is mandatory to have the possibility to prepare and exchange tips *in situ* in a short turn-around time. We use etched tungsten tips coated with 5–100 ML of iron. A typical tip preparation procedure is as follows. The tungsten tip is cleaned by heating it to 2000 K by means of electron bombardment in the preparation chamber. The tip is then sharpened by field emission until a good imaging quality is attained. Iron coating and subsequent annealing is performed in the MBE chamber. This yields a properly imaging tip in about 70% of the cases. Since field emission sharpening most likely results in a throw-off of iron this is no longer recommended at this stage. In a considerable fraction of cases tip preparation has to be repeated. Thus a tip exchange mechanism is indispensable.

Figure 6 shows schematically the assembly. The tip is fixed in a molybdenum tip holder. For inserting a tip into the scanner the tip holder is carried by means of the transporter which can be placed into the sample receptacle where it is positioned such that the tip holder ends up precisely below

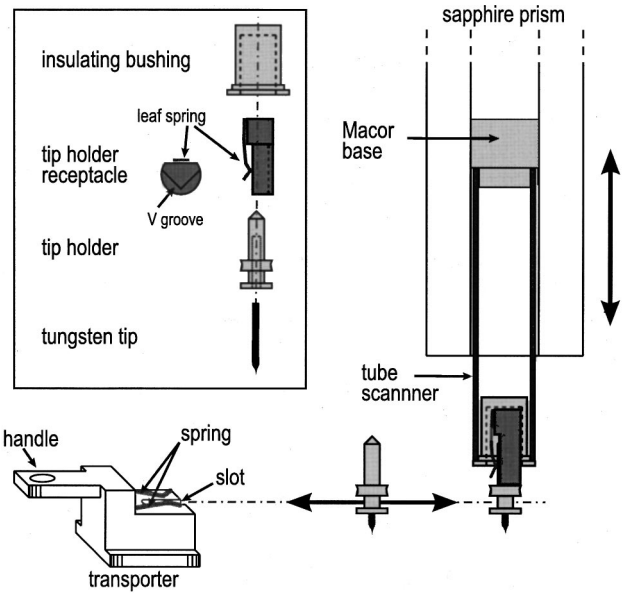

FIG. 6. Schematic drawing of the tip exchange mechanism.

the retracted scanner. Driving down the linear motor lets the tip holder slip into a V-shaped groove of the tip receptacle which is mounted inside an insulating bushing within the lower end of the scanner tube. A small leaf spring clamps the tip holder. Now the transporter can be retracted, leaving holder and tip firmly attached to the scanner tube.

Tip and sample exchange is carried out using a ''Mechanical Hand'' [26] which allows a simple and safe operation. Tip exchange comes down to a matter of minutes, sample exchange being even faster. A whole tip preparation procedure, including fresh coating, accounts to less than one hour.

E. Electrical connections

Since electrical leads introduce heat into the cryostat special attention has to be paid to an optimum of thermal anchoring of all wirings. The leads for the magnet current supply, level meters, and temperature sensors are fed through the top side of the cryostat. They are effectively cooled by the flow of cold helium gas. The microscope wiring, however, is fed directly into UHV via several multipin feedthroughs at the bottom flange of the outer vacuum chamber (see Fig. 1). We use custom made Capton insulated shielded twisted pair VA steel cables with an overall diameter of 1 mm. They are thermally anchored to both the nitrogen and the helium stage (cf. Figs. 1 and 3). At the nitrogen stage every single lead is wound around a copper pole ten of which are mounted on top of a flange and thereby fixed to the base flange of the nitrogen shield. Anchoring to helium temperature is achieved in a similar way: a ten gear thread is cut into the microscope's pedestal such that all ten leads can be firmly wound around it, being held in place by appropriate clamps. When installed, the nitrogen and the helium flange are mechanically disconnected. For maintenance works they get coupled so that they form a unit with the microscope on top. Mounting and dismounting requires approx. 1/2 h.

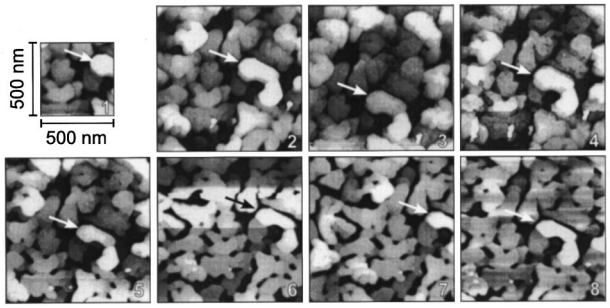

FIG. 7. Sequence of images demonstrating the microscope's ability to regain a microscopic location after a macroscopic movement. Au(111)/Mica, ambient condition. One particular island is marked by an arrow. Each scan was followed by a retraction of the tip by 16 mm, rotation of the sample by 90°, rerotation of the sample, reapproach of the tip. Maximum lateral offset during subsequent scans <280 nm, maximum lateral offset during seven cycles <425 nm.

V. PERFORMANCE

A. Micropositioning

Due to the very high stability of both the linear and the rotational drive one can regain a microscopic location on the sample after a macroscopic movement. This feature is illustrated in Fig. 7. The series of images was taken *ex situ* on Au(111)/mica. Shown are some islands of characteristic shape which can easily be distinguished, one of them being marked by an arrow. After each scan the tip was retracted by 16 mm, followed by a rotation of the sample by 90°, rerotation of the sample, and reapproach of the tip. The maximum lateral offset during subsequent scans was found to be < 280 nm, and < 425 nm during seven cycles.

B. Atomic resolution

Figure 8 shows atomic resolution obtained in UHV on a terbium film grown *in situ* on W(110). The dark sites are caused by adsorbates from the residual gas, probably CO. A profile along the line indicated is shown below the image.

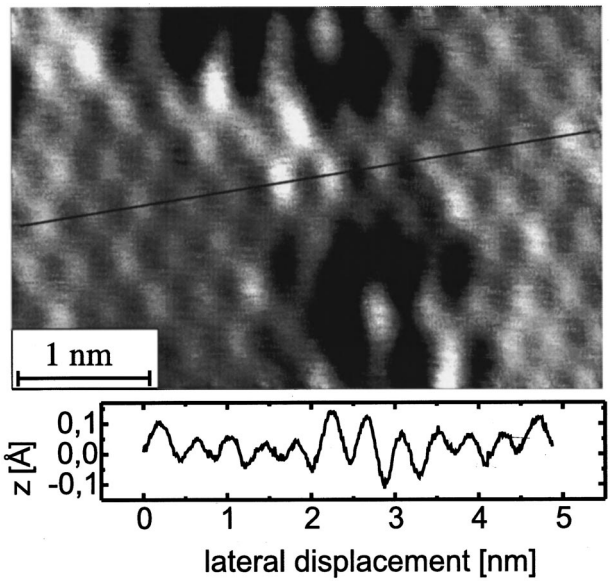

FIG. 8. Atomic resolution on Tb(0001)/W(110) at $T = 16.8$ K. The profile below the image is taken along the line indicated.

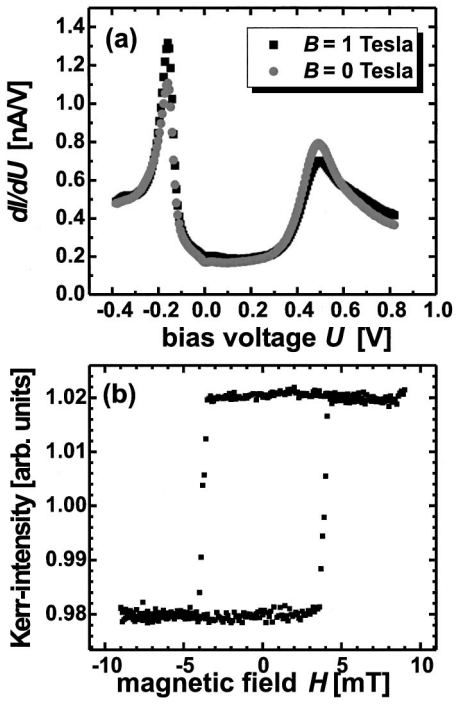

FIG. 9. (a) Impact of an external magnetic field of $B = 1$ T on the spin split surface state of 50 ML Gd(0001)/W(110) as measured with a Fe covered tungsten tip (black squares: field applied; gray circles: no field applied). (b) Kerr loops measured *in situ* on a 50 ML Gd(0001)/W(110) film.

Despite the great length of the scanner the resolution achieved highlights the stability of the whole microscope setup.

C. Spectroscopy of the spin split surface state of gadolinium

We prepared a 50 ML smooth Gd(0001) film by electron beam evaporation on a W(110) single crystal and subsequent annealing. A clean tungsten tip was coated with approx. 100 ML Fe. In a simultaneous measurement at a sample temperature of $T = 16.9$ K topographic, $I(U)$ and $dI(U)/dU$ data were obtained. Figure 9(a) shows two curves of the differential conductivity dI/dU, which is a measure of the local density of states, obtained by a lock-in technique. Black squares indicate the spectrum taken with a magnetic field of $B = 1$ T applied perpendicular to the sample surface, whereas gray circles show the spectrum with no external field applied, i.e., in remanence. Both spectra were measured at exactly the same sample location. The well known spin split Gd surface state is clearly resolved.[8,27,28] By comparing the two spectra one can see the impact of the applied external magnetic field which forces the magnetization of tip and sample into a parallel configuration. The intensity of the occupied part of the surface state at a binding energy $E_{\mathrm{bin}} = -160$ meV is enhanced by 22% at the expense of the unoccupied part, energetically located at a binding energy $E_{\mathrm{bin}} = +500$ meV which is damped by 12.5%. There is no energy shift of the peaks due to the magnetic field. By rotating the sample by 90° [cf. Fig. 5] easy axis Kerr loops [Fig. 9(b)] were measured *in situ* on an identically prepared sample.

ACKNOWLEDGMENTS

We would like to thank M. Getzlaff, S. H. Pan, and J. Podsiadly for useful discussions. Financial support from the DFG (Grant No. Wi 1277/3 and Graduiertenkolleg ''Physik nanostrukturierter Festkörper'') and from GIF (Grant No. I-550-184.14/97) is gratefully acknowledged.

[1] P. Grünberg, R. Schreiber, and Y. Pang, Phys. Rev. Lett. **57**, 2442 (1986).
[2] M. N. Baibich, J. M. Broto, A. Fert, F. Nguyen Van Dau, and F. Petroff, Phys. Rev. Lett. **61**, 2472 (1988).
[3] G. Binasch, P. Grünberg, F. Saurenbach, and W. Zinn, Phys. Rev. B **39**, 4828 (1989).
[4] E. Betzig, J. K. Trautmann, R. Wolfe, E. M. Gyorgy, and P. L. Flinn, Appl. Phys. Lett. **61**, 142 (1992).
[5] J. Kirschner, in *Surface and Interface Characterization by Electron Optical Methods*, edited by A. Howie and U. Valdré (Plenum, New York, 1998).
[6] M. Dreyer, M. Kleiber, A. Wadas, and R. Wiesendanger, Phys. Rev. B **59**, 4273 (1999).
[7] R. Wiesendanger, H.-J. Güntherodt, G. Güntherodt, R. J. Gambino, and R. Ruf, Phys. Rev. Lett. **65**, 247 (1990).
[8] M. Bode, M. Getzlaff, and R. Wiesendanger, Phys. Rev. Lett. **81**, 4256 (1998).
[9] Y. Suzuki, W. Nabhan, and K. Tanaka, Appl. Phys. Lett. **71**, 3153 (1997).
[10] R. Wiesendanger, I. V. Shvets, D. Bürgler, G. Tarrach, H.-J. Güntherodt, J. M. D. Coey, and S. Gräser, Science **255**, 583 (1992).
[11] W. Wulfhekel and J. Kirschner, Appl. Phys. Lett. **75**, 1944 (1999).
[12] S. H. Tessmer, D. J. van Harlingen, and J. W. Lyding, Rev. Sci. Instrum. **66**, 4146 (1995).
[13] J. G. A. Dubois, J. W. Gerritsen, J. G. H. Hermsen, and H. van Kempen, Rev. Sci. Instrum. **66**, 4146 (1995).
[14] Ch. Wittneven, R. Dombrowski, S. H. Pan, and R. Wiesendanger, Rev. Sci. Instrum. **68**, 3806 (1997).
[15] S. H. Pan, E. W. Hudson, and J. C. Davis, Rev. Sci. Instrum. **70**, 1459 (1999).
[16] Omicron Multiprobe *MX*.
[17] Ch. Witt, U. Mick, M. Bode, and R. Wiesendanger, Rev. Sci. Instrum. **68**, 1455 (1997).
[18] Omicron Variable Temperature STM.
[19] Oxford Instruments, Cambridge CB4 4WZ, United Kingdom.
[20] Ceramic Products, Palisades Park, NJ 07650.
[21] S. H. Pan, S. Behler, M. Bernasconi, and H.-J. Güntherodt, Bull. Am. Phys. Soc. **37**, 167 (1992).
[22] M. Bode, M. Hennefarth, D. Haude, M. Getzlaff, and R. Wiesendanger, Surf. Sci. **432**, 8 (1999).
[23] Staveley Sensors, East Hartford, CT 06108.
[24] W. Allers, A. Schwarz, U. D. Schwarz, and R. Wiesendanger, Rev. Sci. Instrum. **69**, 221 (1998).
[25] Lakeshore Cryotronics, Westerville, OH 43081.
[26] Vacuum Generators, Hastings, E Sussex, England.
[27] M. Getzlaff, M. Bode, S. Heinze, R. Pascal, and R. Wiesendanger, J. Magn. Magn. Mater. **184**, 155 (1998).
[28] R. Wiesendanger, M. Bode, and M. Getzlaff, Appl. Phys. Lett. **75**, 124 (1999).